

If you would like us to re-send this article, or any portion of it, please let us know within three working days of receiving it.

Thank you,

The Interlibrary Loan Staff
Fogler Library, University of Maine
Ariel Address: 130.111.64.171
OCLC Symbol: MEU

Borrower: BBH

Lending String: *MEU,WLU,CKM,HVC,AMH

Patron: Olins, Ada

Journal Title: The molecular biology of the mammalian genetic apparatus ; [proceedings] /

Volume: Issue:
Month/Year: 1977**Pages:** 211-237

Article Author: International Symposium on the Molecular Biology of the Mammalian Genetic Apparatus; Its Relationshi

Article Title: Olins, Breillat, Carlson, Senior, Wright, Olins; On nu models for chromatin structure

Imprint: Amsterdam ; New York ; North-Holland Pub

Call #: QH426 .I6 1975 v.1

Location: ORO stacks AVAILABLE

Mail Charge
Maxcost: 45.00IFM

Shipping Address:
Library, ILL
Bowdoin College
LIBRARY / ILL DEPT
3001 College Station
Brunswick, ME 04011-8421

Fax: ill@bowdoin.ed
Ariel: 139.140.112.4
Odyssey: 139.140.13.32

ILLiad TN: 101733



ILL Number: 54605501



University of Maine
Interlibrary Loan

ON NU MODELS FOR CHROMATIN STRUCTURE

A.L. OLINS, J.P. BREILLATT, R.D. CARLSON, M.B. SENIOR*,
E.B. WRIGHT and D.E. OLINS

*From The University of Tennessee-Oak Ridge School of Biomedical Sciences, The Biology Division,
Oak Ridge National Laboratory, and the Molecular Anatomy Program, Oak Ridge National
Laboratory, Oak Ridge, Tennessee 37830, U.S.A.*

'You boil it in sawdust: you salt it in glue:
You condense it with locusts and tape:
Still keeping one principal object in view--
To preserve its symmetrical shape'

Lewis Carroll
The Hunting of the Snark (1876)

Introduction

The idea that chromatin might possess a periodic structure developed from the early X-ray scattering studies of Wilkins and co-workers [1,2] and those of Luzzati and Nicolaieff [3,4]. Prior to 1973, the most widely accepted model for the DNA folding in chromatin was that of Pardon and Wilkins [5], which assumed: A uniform distribution of histones along the DNA, and a superhelical folding of the nucleohistone fiber, with a DNA length packing ratio of $\sim 3:1$. Independent electron microscopic studies of chromatin had failed to indicate any unequivocal periodic structure, although classes of chromatin fiber diameters could be clearly discerned. Generally, the spreading of chromatin fibers on a water surface, at low ionic strength and in the presence of a chelator, resulted in fibers of approximately 100 Å diameter, while other solvent conditions promoted the appearance of

* Present address: Department of Microbiology, University of Pennsylvania School of Medicine, Philadelphia, Pennsylvania.
Research supported by the Energy Research and Development Administration under contract with Union Carbide Corporation.

200–250 Å diameter chromatin fibers [6,7,8]. In 1973 employing techniques modified from those of Miller and co-workers [9,10], we [11] and Woodcock [12] independently observed an ultrastructural basis for chromatin periodicity. Simultaneously, biochemical studies of the products of nucleolytic attack of chromatin furnished the basis of isolation and characterization of this newly described chromatin subunit [13,14].

The present paper, which emphasizes the work in progress in our laboratory, is divided into four parts: a) visualization of the chromatin subunits (the nu or v bodies) in freshly spread nuclei; b) isolation and characterization of monomer v bodies; c) speculations about the internal structure of v bodies; and d) reflections on the higher-order packing of v bodies in chromatin.

Visualization of the chromatin subunits

The reader must examine the following electron micrographs with a degree of caution, particularly as outlined in fig. 1.

When isolated nuclei are exposed to solvents of varying ionic composition, alterations in nuclear volume and chromatin condensation can be readily observed [15,16,17,18]. In particular, nuclei swell and lose their granularity in low ionic strength solvents devoid of divalent cations, probably as a consequence of

THE MICROSCOPE Made Easy:

OR,

I. The Nature, Uses, and Magnifying Powers
of the best Kinds of MICROSCOPES
Described, Calculated, and Explained:

FOR THE

Instruction of such, particularly, as desire to search
into the WONDERS of the Minute Creation,
tho' they are not acquainted with Optics.

Together with

Full Directions how to prepare, apply, examine, and preserve
all Sorts of OBJECTS, and proper Cautions
to be observed in viewing them.

II. An Account of what surprizing Discoveries
have been already made by the MICROSCOPE:
With useful Reflections on them.

AND ALSO

A great Variety of new Experiments and Observations,
pointing out many uncommon Subjects for the
Examination of the CURIOUS.

By HENRY BAKER, Fellow of the Royal Society,
and Member of the Society of Antiquaries, in London.

Illustrated with COPPER PLATES.

Resum Naturæ vulgaris magis quàm in Minutis res est.
PLIN. Hist. Nat. Lib. XI. c. 2.

LONDON:

Printed for R. DODDLEY, at Tully's Head in Pall-Mall.
M. DC. CXLII.

[62]

CHAP. XV.

Cautions in viewing Objects.

Beware of determining and declaring your
Opinion suddenly on any Object; for
Imagination often gets the Start of Judg-
ment, and makes People believe they see
Things, which better Observations will con-
vince them could not possibly be seen: there-
fore assert nothing till after repeated Experi-
ments and Examinations in all Lights and in
all Positions.

When you employ the Microscope, shake
off all Prejudice, nor harbour any favourite
Opinions; for, if you do, 'tis not unlikely
Fancy will betray you into Error, and make
you think you see what you would wish to
see.

Remember that Truth alone is the Mat-
ter you are in search after; and if you have
been mistaken, let not Vanity reduce you to
persist in your Mistake.

Pass no Judgment upon Things over-ex-
tended by Force, or contracted by Dryness,
or in any Manner out of their natural State,
without making suitable Allowances.

There is no Advantage in examining any
Object with a greater Magnifier than what
shews the same distinctly; and therefore, if
you can see it well with the third or fourth
Glas,

Fig. 1. Advice of an experienced 18th Century microscopist.

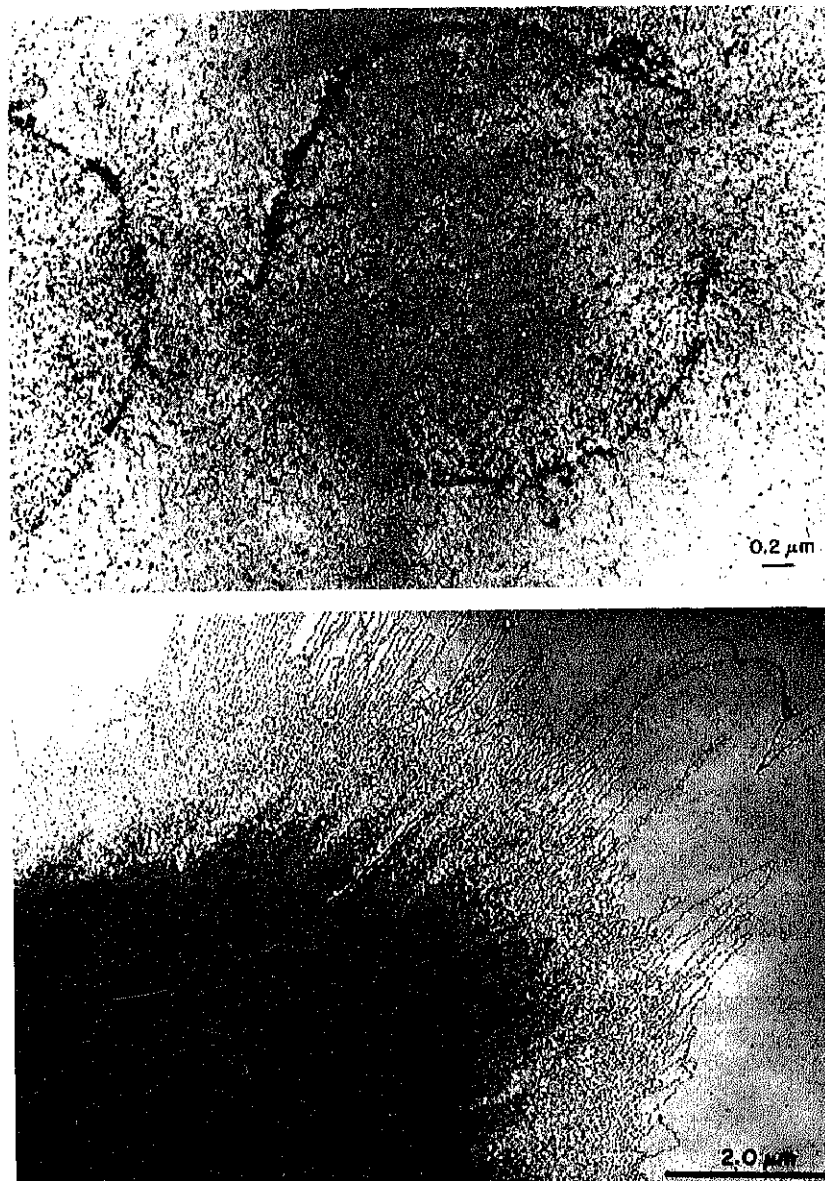


Fig. 2(above) Electron micrograph of a thin section of a water-swollen chicken erythrocyte nucleus. Specimen preparation, embedding and staining as described previously [18]. 15,000 ×. (below) Electron micrograph of a swollen and fixed chicken erythrocyte nucleus centrifuged onto a glow-discharged carbon-coated grid, dried in Photo-Flo, and dried in 0.5% ammonium molybdate (pH 7.4). The chromatin fibers spilling out of the nucleus are well separated at the perimeter of the nucleus. 22,000 ×.

electrostatic repulsion between the polyanionic chromatin fibers. In extreme conditions (e.g., distilled water after chelation or displacement of divalent cations), the nucleus literally explodes, with chromatin fibers streaming into the solvent. Electron microscopic studies of thin sections of fixed, water-swollen nuclei [19,20] reveal very little discernible structure (fig. 2a); the separated chromatin fibers exhibit diameters of approximately 70–100 Å. Because the chromatin fibers extend in all directions, only short segments can be observed in the thin sections. If the fixed water-swollen nuclei are centrifuged onto a carbon-coated microscope grid, dried in Kodak Photo-Flo [9,10], and subsequently dried in dilute stains [21,22,23], the chromatin fibers appear as long, unbranched strands (fig. 2b). At higher magnification the chromatin fibers can be resolved into linear arrays of spheroid particles with ~ 80 Å diameter (the ν bodies), joined by connecting strands, ~ 20 Å thick (fig. 3 and 4). The ν bodies frequently reveal characteristic internal structure: a dot of stain in the particle center; a line of stain partly or completely across the particle diameter. The dimensions of the ν body and the existence and length of the connecting strand have furnished some basis for controversy in the field. Observations compiled from a number of studies are presented in table 1, which also illustrates the widespread occurrence of the chromatin particulate structure. Differences in reported ν body diameters probably reflect variations in particle distortions due to dehydration, variations in penetration of stain, calibration of magnification, and calculated corrections of heavy metal deposition. As an example of the difficulty of estimating hydrated dimensions, the volume of ribosomal particles decreases $\sim 50\%$ due to the dehydrating condition of electron microscopy [31]. Furthermore, it is likely that the hydrated ν bodies would have a diameter ~ 100 – 110 Å, in order to explain features of the low-angle X-ray scattering (see below). The significance of the connecting strand remains to be completely clarified. We have argued [21,22] that the packing of ν bodies seems to be sensitive to stretching, and that one frequently observes a mixture of close-packed and stretched linear arrays of particles. Although the stretched configuration may well be artifactual, we maintain that, in certain circumstances, it can also be informative. Under certain staining conditions (table 1 [23,26,27]) the connecting strands exhibit reproducible lengths (i.e., histograms of strand lengths exhibit clear peak values). It is probable that this is an unravelled segment of the particle DNA, and represents a less tightly bound portion of defined length. With respect to the data from spread chicken erythrocyte nuclei [23], a connecting strand of ~ 140 Å would be equivalent to ~ 40 – 60 nucleotide pairs of native DNA.

As shown in table 1, the ν body structure of chromatin seems to occur in many different types of eukaryotic nuclei, a conclusion that agrees with studies on the DNA fragments obtained after nuclease digestion (see below). It further seems likely that the particulate structure is not dictated by a unique nucleotide sequence, since isolated histones can be reconstituted with a variety of different

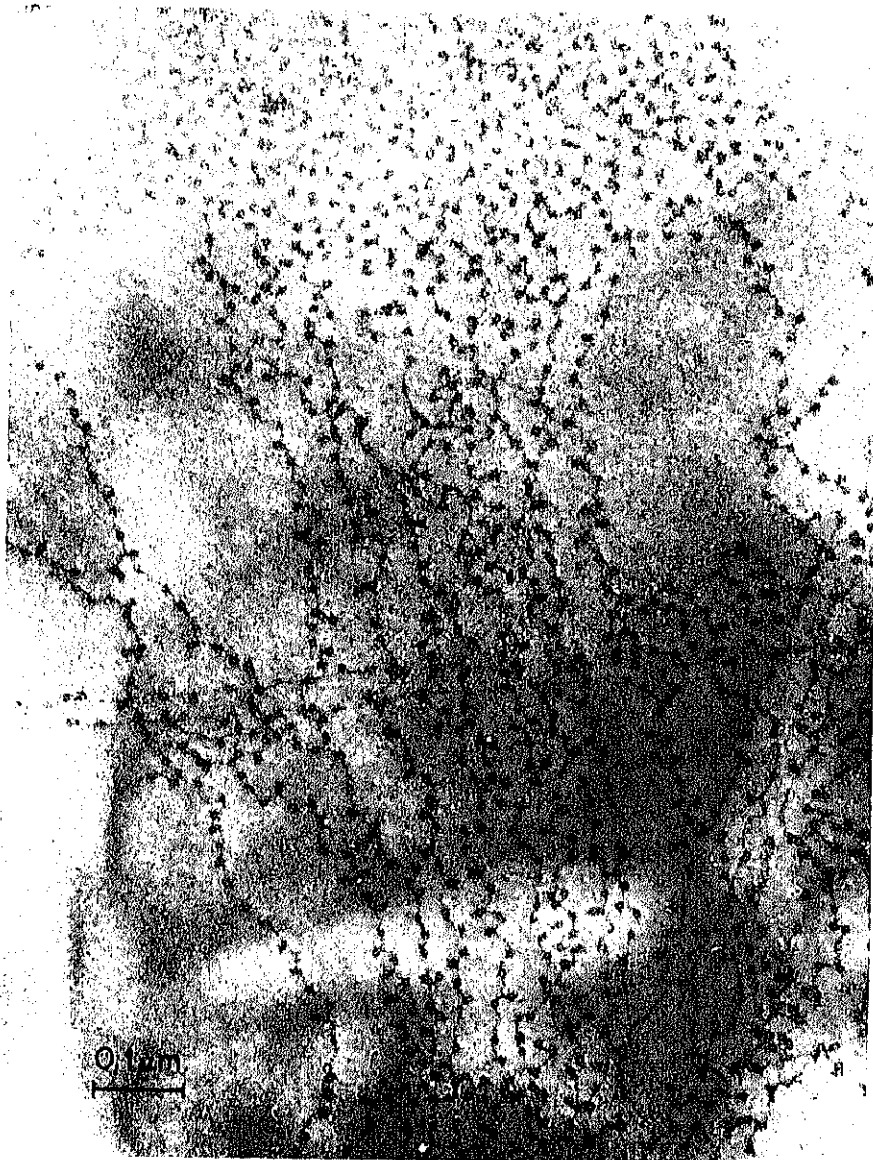


Fig. 3. Electron micrograph of a spread of a chicken erythrocyte nucleus. The regularity of the connecting strand length can be readily visualized. Specimen preparation similar to fig. 2b, except that the sample was dried in 0.2% uranyl acetate dissolved in methanol. 125,000 \times .

DNA molecules (e.g., *E. coli*, T7 and T4 DNAs [23]; and adenovirus [28] DNA); to yield ν bodies of similar morphology. From such evidence and from numerous studies on histone-histone interactions (see the section on Internal structure of ν bodies) it appears that the foundations of the particulate subunit

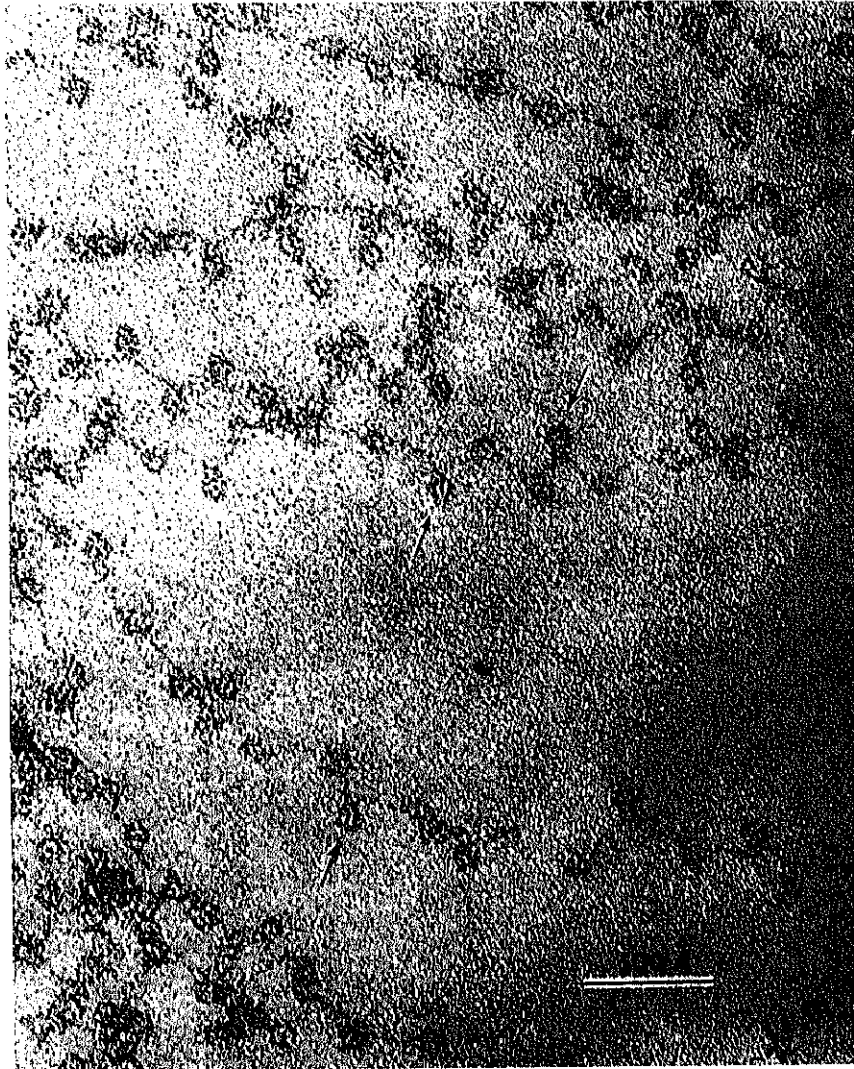


Fig. 4. High resolution micrograph of spread chicken erythrocyte nucleus. The arrows point to v bodies with clear internal structure. Many chromatin fibers exhibit a zig-zag configuration with the v bodies lying on alternate sides of the connecting strand. Specimen preparation similar to fig. 2b. except that the sample was dried in aqueous 0.2% uranyl acetate. 350,000 \times .

structure of chromatin are specific histone-histone interactions combined with more general interactions between histone and DNA.

The emerging conception of chromatin as 'beads-on-a-string' is not completely new. The eccentric French artist Jean Ignace Isidore Gerard Grandville (1803-1847) held remarkably similar views (fig. 5).

TABLE 1
Dimensions from electron microscopic studies.

Source	v Bodies diameter (Å)	Edge-to-edge connecting strand (Å)	Stain technique	Reference
Chick RBC	60-80	—	Positive and negative	11,22
Calf thymus	70-100	—	Positive and negative	12,24
Rat liver	74	240	Negative	25
Amphibian and Avian RBC	81	140	Negative	23
Chick RBC	89	250	Negative	26
Mitotic CHO	70-90	300	Positive and negative	27
Mitotic L cells	125	—	Shadow	28
Calf thymus (depleted of histone 1)	109	134	Shadow	29
SV-40	135 × 50	128	Dark field	30
Calf thymus				

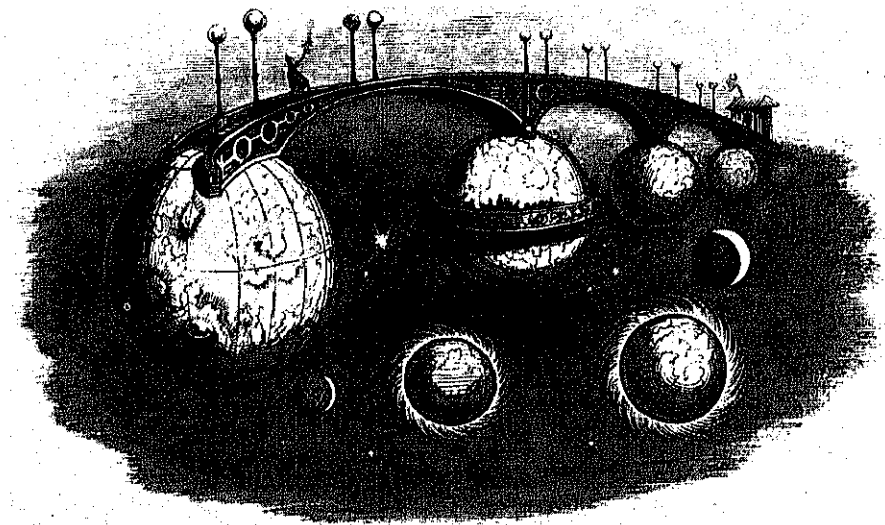


Fig. 5. *The Planet Bridge* by J.I.I.G. Grandville (1844), in *The Mysteries of Infinity. Un Autre Monde*.

Isolation and properties of chromatin ν bodies

Although small quantities of monomer ν bodies can be isolated by ultracentrifugation of water-swollen, fixed and sonicated nuclei [32], the method of choice for particle isolation involves nuclease digestion of isolated nuclei or chromatin [33,13,14], followed by ultracentrifugal fractionation of the digested products [34,35]. The kinetics of digestion of chicken erythrocyte nuclei with micrococcal nuclease is shown in fig. 6a. It is clear that as digestion proceeds, there is an increase in slowly sedimenting material, and a decrease in rapidly sedimenting material, in agreement with the results of other investigators [36,37]. In order to obtain a high yield of monomer particles (ν_1) for physical characterization, one hour digests of chicken erythrocyte nuclei were fractionated by zonal ultracentrifugation (fig. 6b). In the experiment, approximately 1/3 of the rotor capacity was used, and approximately 30 mg of monomer particles (ν_1) were obtained. In this run, the purity of the monomers (pool 1) was $\sim 90\%$; dimers (pool 2) and trimers (pool 3), about 60%. Recentrifugation of dimers and trimers on smaller sucrose gradients (SW 41 rotor) was occasionally employed for further purification.

The preparation of even larger quantities of monomer ν bodies is desirable for attempts at crystallization, and for light, X-ray and neutron scattering studies. Employing the K-VIII zonal rotors in a K series centrifuge [41], we have recently isolated ~ 1.0 gram of nuclease digested monomer ν bodies (fig. 7).

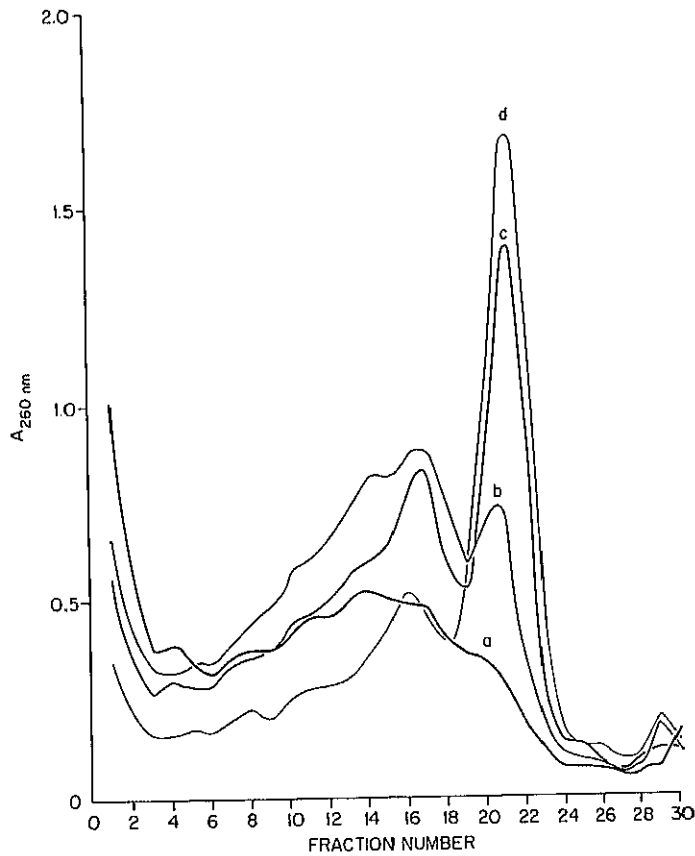


Fig. 6. a) Fractionation of micrococcal nuclease digested chicken erythrocyte nuclei by sucrose gradient ultracentrifugation - the effects of time of digestion. Chicken erythrocyte nuclei were isolated according to the procedure of Van Lente et al. [35]. Five ml of chicken blood were collected in 30 ml of buffer containing 10 mM NaCl, 10 mM Tris-HCl, and 3 mM $MgCl_2$, pH 7.4 (STM buffer). Cells were pelleted at low speed (10 min, ~ 4000 g) and lysed at 4 C in STM buffer with the addition of 0.5% Nonidet P40 (Particle Data Lab Ltd., Elmhurst, Ill.) (STMN buffer). Nuclei were washed 3 times and resuspended in STMN buffer to a concentration of $\sim 1.4 \times 10^9$ nuclei/ml. The solution was made 10^{-4} M in $CaCl_2$, and samples were incubated at 37 C for various times with 60 $\mu g/ml$ Micrococcal Nuclease (Worthington Biochemical Corp.). The digestion was stopped by the addition of ice cold EDTA (pH 7.0) to 40 mM, followed by sonication for 2-3 min at 0 C (setting 8, Biosonik (Bronwill Scientific, Rochester, NY)), and centrifugation at low speed. (Most recently, we have eliminated the sonication step, with no ill effects.) The pellet was dispersed in 0.2 mM EDTA, pH 7.0 (final $A_{260} \sim 50-100$). Ten to twenty lambda of the dispersed pellet was layered on the top of 5-20% linear sucrose gradients (0.2 mM EDTA, pH 7.0), and centrifuged in a Beckman Spinco SW41 rotor spun at 35,000 rpm for 12 h at 4 C. Gradients were fractionated from the bottom of the centrifuge tubes. Digestion times: (a) 10 min; (b) 30 min; (c) 1 h; (d) 2 h.

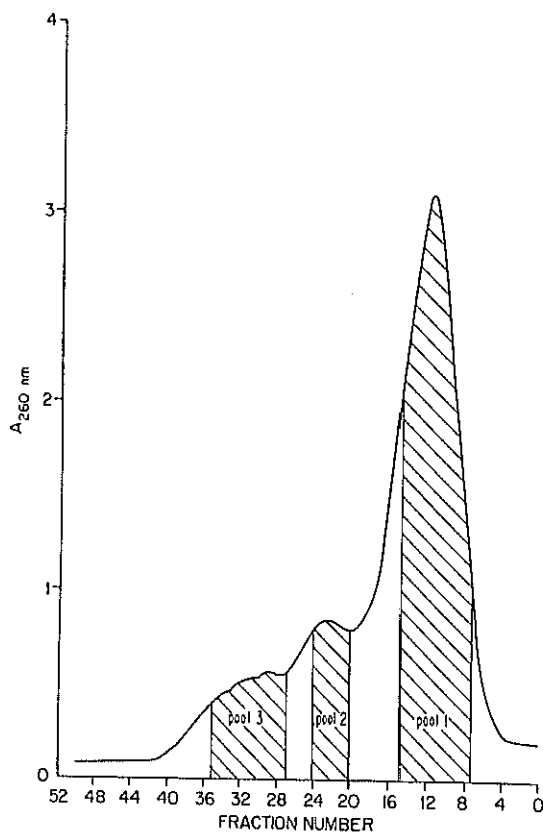


Fig. 6. b) Fractionation of micrococcal nuclease digested chicken erythrocyte nuclei by zonal centrifugation - the Beckman Ti-15 zonal rotor. Preparative isolations of nuclease-resistant chromatin particles were performed in a Beckman Ti-15 zonal rotor by the following protocol: at 3 C and 1500 rpm, 950 ml water overlay was rapidly introduced through the edge line; then 15-20 ml sample, containing digested chromatin at approximately 5 mg/ml in 3% w/v sucrose, and 0.2 mM EDTA, was metered in the edge line at 15 ml/min and followed immediately by the light end of an 8.6-15% w/w sucrose gradient containing 0.2 mM EDTA (pH 7.0). The 500 ml linear-with-volume gradient was produced by a cam-programmed Beckman gradient former, and after the first 4 min the loading rate was increased from 15 ml/min to 40 ml/min. A cushion of 17.5% w/w sucrose filled the remainder of the rotor cavity. After centrifugation for 5-6 h at 32,000 rpm ($w^2t = 2.0-2.4 \text{ sec} \times 10^{11}$) the rotor contents were displaced through the center line and the chromatin collected in 15 ml fractions. This separation protocol is derived from that developed for isolation of macroglobulin from plasma [38,39], and further optimized through use of the simulation program DIFED [40]. Fractions from the zonal rotor were monitored at 260 nm, and pools containing predominantly monomer, dimer and trimer particles were concentrated in a collodian bag apparatus (Schleicher and Schuell Co., Keene, NH) to an A_{260} of $\sim 50-100$.

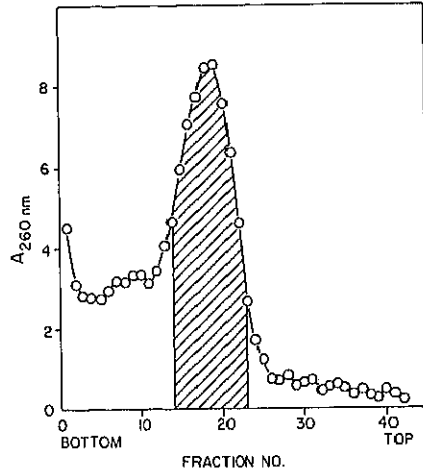


Fig. 7. Fractionation of micrococcal nuclease digested chicken erythrocyte nuclei by zonal centrifugation - the K-VIII rotor. For the very large scale production of monomer ν bodies, 8 chickens were exsanguinated, the blood (540 ml) collected into 60 ml of Anticoagulant Citrate Dextrose (Aminco, Silver Springs, MD) to prevent clotting. The blood was filtered through gauze, diluted with 300 ml STM buffer, and centrifuged for 15 min at 400 g. The loose erythrocyte pellet was suspended in 1.5 l of STMN buffer, stirred with a magnetic bar for 10 min and centrifuged; the entire washing cycle was repeated a total of 4 times. The resulting nuclear preparation was diluted to a concentration of 1.4×10^9 nuclei/ml (860 ml), made 10^{-3} M CaCl_2 , and micrococcal nuclease added to 6 μg enzyme/ml. Digestion conditions were 6-8 h, 37 C with occasional shaking. The reaction was terminated by addition of 174 ml of 200 mM EDTA and rapid chilling. After centrifugation (15 min, 600 g), the digested nuclear pellet was resuspended in 120 ml of 0.2 mM EDTA, stirred and brought to final concentration of ~ 10 mg digested chromatin/ml (i.e., $A_{260} \sim 100$) in 4% sucrose.

For fractionation in the K-VIII rotor a 4.5 l overlay of 2.8% sucrose, 0.2 mM EDTA was introduced into the static rotor through the bottom line; followed by the ~ 200 ml sample; and subsequently by a 12-30% w/w sucrose gradient also containing 0.2 mM EDTA. This 3:1 gradient was formed by a gradient maker with a 3.6 l mixing chamber [42]. A 750 ml cushion of 34% w/w sucrose, 0.2 mM EDTA completed filling of the 8.45: rotor cavity. The rotor contents were reoriented into the spin configuration according to a controlled acceleration protocol, and centrifuged at 35,000 rpm for 10 h at 13 C. The rotor was decelerated under control and the gradient collected in 100 ml fractions from the bottom line of the static rotor. The monomer fraction was concentrated by precipitation with 10 mM MgCl_2 in a 1 l graduate cylinder overnight at ~ 4 C. The supernatant was gently removed by suction; the pellet further concentrated by centrifugation. The loose pellet of monomers (~ 50 ml) was subsequently dialyzed against 5 l each of 20 mM, 2 mM and 0.2 mM EDTA. The final product was an almost clear solution (~ 60 ml) of particles ($A_{260} \sim 157$). For ultimate purification of monomer ν bodies it may be necessary to recycle the preparation in the K-VIII zonal rotor one more time.

Table 2 contains a summary of published physical data on chromatin monomer particles, and includes the results of our physical studies on two separate zonal (i.e., Ti-15 rotor) preparations. Most of the published data on monomer DNA-fragment size come from gel electrophoresis of DNA which was prepared

TABLE 2

Physical properties of chromatin fragments resembling v bodies.

Particles			DNA		
Protein					
DNA	Mol. wt.	Source	Mol. wt.	Base pairs	References
1.22	295,000	Chick erythrocytes	141,000*	(210)	32
1.3	(315,000)	Rat liver	(137,000)	205	34
1.2	(295,000)	Trout testis	(134,000)	200	43
1.39	(296,000)	Duck reticulocytes	(124,000)	185	44
—	—	Rat liver	(124,000)	185	45
—	—	Rat liver	120-150,000	(201)	46
—	—	Calf thymus	(117,000)	110-175	47
—	—	Trout testis	(117,000)	175	43
—	—	Pea seed	(114,000)	170	48
—	—	Mouse myeloma			
—	—	Rat liver	(114,000)	170	34
—	—	Rat liver	(107,000)	160	45
1.39	(225,000)	Duck reticulocytes	(94,000)	140	44
—	—	Yeast	(90,000)	135	49
—	—	Calf thymus	70-80,000	110-120	25
—	—	Calf thymus	80,000	120	36
1.64	(223,000)	Chick erythrocytes	85,000*	(126)	50
1.78	(224,000)	Chick erythrocytes	80,000*	(120)	50
1.86	(230,000)				

* DNA was prepared from isolated chromatin particles by digestion for 1 h at 37 C with 1 mg/ml Pronase (pre-incubated for 15 min at 37 C) in a solvent containing 0.5% SDS and 1 M NaCl. The DNA was further purified by extracting 3 times with an equal volume of buffered phenol, and 1 time with ether. Dissolved ether was evaporated with N₂ and the DNA was either precipitated with 2 volumes of ethanol at -20 C overnight, or exhaustively dialyzed vs appropriate solvents. For molecular weight determination by analytical ultracentrifugation DNA isolated from purified monomer was exhaustively dialyzed vs SSC (0.15 M NaCl, 0.015 M NaCitrate, pH 7.5) and sedimented to equilibrium in a Beckman Model E analytical ultracentrifuge, equipped with absorption optics and a multiplexer attachment. Scans were taken after at least 60 h of centrifugation, and calculations were performed as described [33].

following micrococcal nuclease digestion of isolated nuclei. Such studies indicate that micrococcal nuclease rapidly fragments chromatin to particles containing from 185 to 205 base pairs (and higher multimers). Simultaneously, or very shortly thereafter, DNA fragments of from 140 to 175 base pairs appear, followed by a limit digest of smaller DNA pieces [51,52]. Furthermore, under some con-

ditions of digestion, non-zero background absorbances between the major bands on DNA gels are apparent [44,50], indicating a certain amount of heterogeneity in the DNA cleavage sites.

Monomer particles isolated in the present study have average DNA contents of approximately 120 to 126 base pairs, as determined by sedimentation equilibrium studies. DNA gel electrophoresis of samples from the first zonal preparation (pool 1) indicate the presence of up to 10% of lower molecular weight DNA fragments (data not shown). Although no heterogeneity was apparent from the sedimentation equilibrium profiles of pool 1 DNA fragments, the presence of low molecular weight pieces could lower the measured molecular weight.

Bouyant densities of HCHO-fixed v_1 in CsCl indicated a heterogeneity in protein/DNA for these nuclease monomers. In both preparations listed in table 2, the bands in CsCl were broader than that calculated for a homogenous preparation of similarly-sized particles, and in the second preparation of pool 1, the broad band appeared to be split into at least two peaks.

Electron micrographs of zonal pools 1, 2, and 3 are shown in fig. 8. The appearance of these monomer, dimer and trimer particles in the electron microscope is identical to the appearance of v bodies in spread chromatin fibers (see below).

The electrophoretic pattern of the proteins extracted from purified monomers (v_1), dimers (v_2) and trimers (v_3) are shown in fig. 8D, along with the profiles from intact nuclei, total nuclease digests, and histone standards. There is a small quantity of non-histone protein visible in the intact nuclei isolated by the present procedure, with diminishing amounts present in the total digest, and only trace quantities in the isolated pools. This confirms earlier suggestions [32] that non-histone proteins are not integral components of v bodies. The molar ratios of the histones within these samples (from a single zonal preparation) are given in table 3. Each sample was examined on long (25 cm) SDS gels and average values are shown. Extracts of total undigested nuclei yielded approximately equimolar ratios of the H4, H3, H2a, H2b, and H5. We have repeated this observation on two other preparations of chicken erythrocyte nuclei and estimate that the equimolar ratios are accurate to $\pm 10-20\%$. This observation of the approximate equimolarity of the major classes of histone is consistent with our earlier suggestions on the histone stoichiometry of chromatin v bodies [11,21]. It is not in agreement, however, with previous measurements in our laboratory on the histone molar ratios of acid extracts of intact erythrocyte nuclei [54]. By comparing the yield on SDS gel electrophoresis of histones extracted from identical numbers of intact nuclei by acid treatment (0.25 NH_2SO_4 followed by ethanol precipitation) versus extraction with SDS-mercapto-ethanol, we have determined that SDS extraction results in yields that are 3-4 times greater than with extraction by acid. The earlier measurements [54] appear to have been based upon incomplete extraction. It should be noted that most of the relative histone

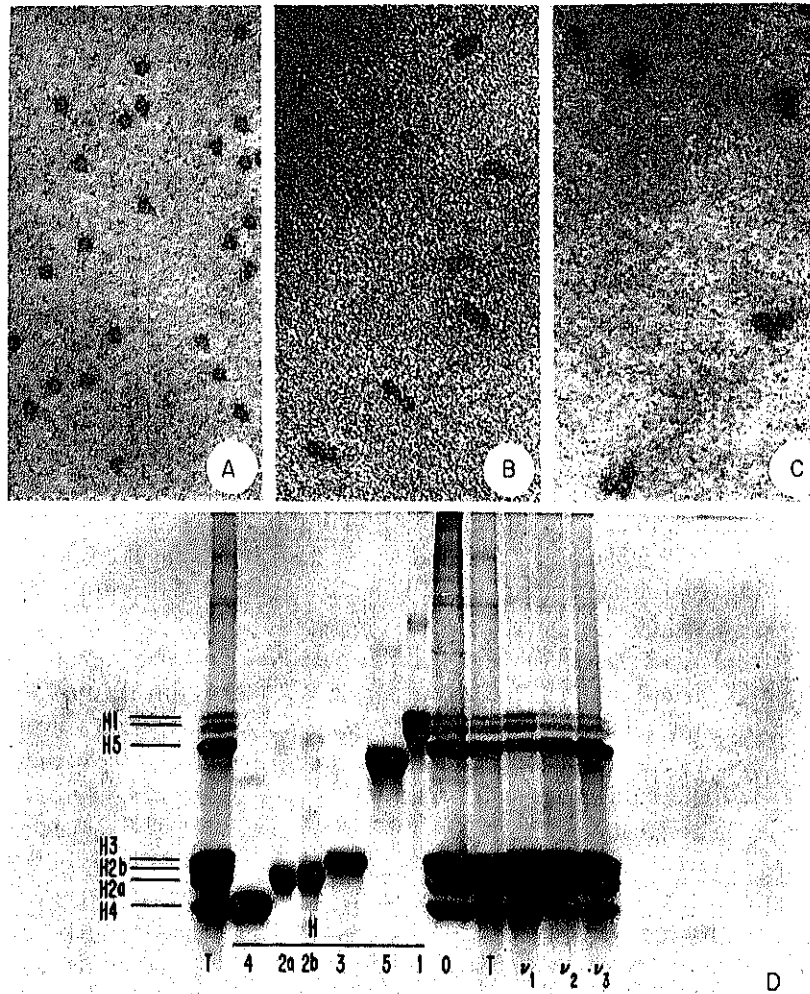


Fig. 8. A,B,C) Electron micrographs of fractions from zonal ultracentrifugation (see fig. 6): A) pool 1; B) pool 2; C) pool 3. One drop of the unfixed particles ($A_{260} \sim 1-2$) was applied to a charged carbon-coated grid, washed and dried in dilute Kodak Photo-Flo, stained and dried in 0.2% aqueous uranyl acetate. $149,000 \times$. D) Gel electrophoresis in sodium dodecyl sulfate, comparing purified chicken erythrocyte histones (H4, H2a, H2b, H3, H5 and H1) with extracts of undigested nuclei (0), micrococcal nuclease digested nuclei (T), and monomer, dimer and trimer fractions (v_1 , v_2 , v_3). Gel electrophoresis conditions were modified from [53], except that gels were 3 mm thick and 120 mm long. Following electrophoresis the gels were stained with 0.1% Amido Black and destained until the background was uniform [54].

ratio data in the literature are based upon acid-extracted nuclei or chromatin [55,56]. The present results, documenting the equimolarity of the histones, would appear to indicate that, for the chicken erythrocyte nucleus at least, the very

TABLE 3

Molar ratios of histones. Proteins were extracted from undigested nuclei by addition of 1/5 volume of 5 × sample buffer (0.3125 M Tris (pH. 6.8), 10% SDS, 25% β-mercaptoethanol, 50% glycerin, 0.005% bromophenol blue) to a solution containing 1–2 mg DNA/ml. Concentrated solution of v_1 , v_2 , and v_3 particles (in 0.2 mM EDTA) or of histone standards (in water [54]) were diluted with appropriate volumes of 5 × sample buffer. Samples were not boiled, since boiling was occasionally observed to lead to precipitation of proteins. Gels were stained in 0.1% Amido Black and destained as previously described [54]. The destained gels were scanned with a Zeineh Soft Laser Scanning Densitometer (Biomed. Industries, Inc., Chicago, Ill.), equipped with an integrator pen which was used to quantitate the amount of stain in each gel band. By combining data on the relative molar staining of the pure histones with measurements of the relative staining of histone extracts, we were able to estimate the molar ratios of the histones in the extracts of undigested nuclei, and of monomer, dimer and trimer fractions (see [54] for the details of the calculations).

Histone	Undigested chicken erythrocyte nuclei	Monomer v_1	Dimer v_2	Trimer v_3
H4	1.00	1.00	1.00	1.00
H3	1.01	0.64	0.69	0.64
H2a	0.94	0.87	0.93	0.78
H2b	1.15	0.87	0.92	0.96
H5	0.92	0.35	0.75	0.98
H1	0.45	0.27	0.24	0.26

lisine-rich histones (H5 and H1) are not half-molar with respect to H4 [57]. Obviously, additional measurements on other types of nuclei are necessary. Analysis of histone extracts from zonal fractions enriched with monomer, dimer and trimer v bodies reveal some differences from histone equimolarity (table 3). The most obvious and reproducible difference, compared to undigested nuclei, was a loss of $\sim 2/3$ of H5 in v_1 fractions. The decrease in H3 compared to undigested nuclei was not consistently observed in other experiments. Other investigators have reported monomer particles which are either deficient in [37,43], or entirely lacking [36,58], histone H1, and it is likely that H5 serves some of the same functions in erythrocytes as H1 does in other nuclei. It is not surprising, then, that H5 is preferentially lost during digestion of chicken erythrocyte nuclei. The suggestion has been made that H1 (or H5) is associated with interparticle regions in chromatin (i.e., covering the connecting strands visualized in spread chromatin) [58]. It is interesting to note, therefore, that nuclease-digested monomers (v_1), when air-dried from Photo-Flo, generally do not exhibit any 'tails' in the electron microscope, suggesting that the connecting strands have been digested. That all of the H1, and approximately 30% of the H5, remains with the isolated monomeric v -bodies may reflect weak interactions of these histones with the particle structure. Histone stoichiometry data (table 3) suggest that most of the released

H5 molecules do not associate with multimer particles. Buoyant densities indicate that only 5% of the multimer fractions have protein/DNA higher than the bulk of chromatin. H1 has been found at the top of sucrose gradients of nuclease digests [43], consistent with a partial release of H1 during digestion. The solubility properties of isolated monomer ν bodies strongly resemble those of native chromatin [39]. Preliminary studies in our laboratory indicate that quantitative precipitation of ν bodies can be accomplished by making the fragments in 10 mM MgCl_2 (fig. 7, legend). The precipitate readily redissolves on subsequent dialysis against EDTA solutions. Analysis of the histone content of the resolubilized monomer particles reveals a total absence of H1 and H5 histones. Previous studies on isolated chromatin have indicated that as much as 100 mM MgCl_2 is necessary to displace the very lysine-rich histones [59], further indicating the weaker binding of H1 and H5 following nuclease digestion.

Isolated monomer ν bodies can reveal certain properties observed for intact chromatin. If the particles are made 5 mM MgCl_2 and examined in a phase light microscope, they reveal fibrous aggregates that resemble chromatin examined under similar conditions (fig. 9A). When such aggregates of monomer particles are pelleted by ultracentrifugation and examined by low-angle X-ray scattering, the characteristic chromatin pattern (i.e., $\sim 110, 55, 37 \text{ \AA}$) is observed (fig. 9B).

The facility of reconstructing ν bodies from its dissociated components, i.e., histones and DNA, described earlier, can also be accomplished with the isolated monomer ν bodies. On the basis of electron microscopy, sedimentation behavior and melting temperature, we have obtained almost complete reassociation when an aliquot of ν_1 was dissociated by dialysis against 3 M NaCl, and reconstituted

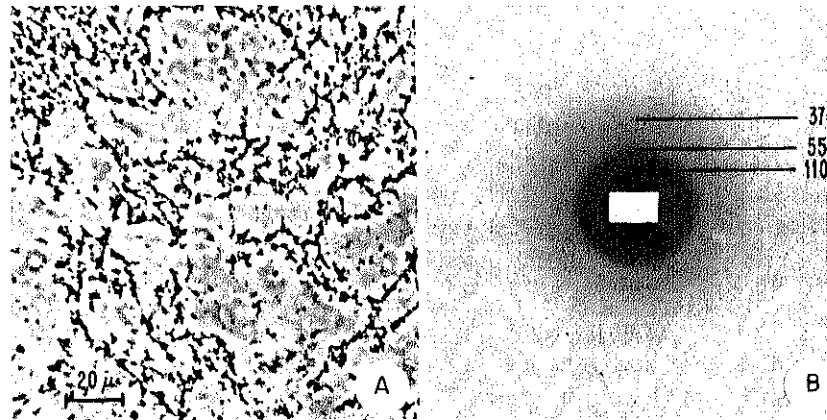


Fig. 9. The effects of adding Mg^{2+} to isolated monomer ν bodies. A) Monomers ($A_{260} \sim 3$) made 5 mM MgCl_2 and examined in the phase light microscope. $370\times$. B) Low angle X-ray diffraction pattern of a centrifuged pellet of ν_1 made 5 mM MgCl_2 . Centrifugation conditions: type 65 rotor, 18 h, 58,000 rpm, 0°C . X-ray exposure (72 h) with Frank optics; sample-film distance, 92 mm.

by stepwise dialysis against buffers containing decreased concentrations of NaCl by techniques employed previously [23].

Internal structure of ν bodies

High resolution electron micrographs of nuclear spreads and isolated particles suggest the existence of characteristic internal structure (fig. 10 and [23]). In the absence of additional data (e.g., images of individual particles observed at different tilt angles; analysis of the types of binding sites for stain), interpretation of the micrographs in terms of histone arrangement within ν bodies can be only highly speculative. Two recent reviews on the 'Quaternary structure of proteins' [60] and on 'Electron microscopy of proteins' [61] discuss the symmetry properties of macromolecules, furnish a goal for the analysis of ν bodies, and stimulate us to formulate ideas of possible histone arrangements within the ν body. We will, therefore, suggest a conception of particle internal structure, intended as a working model. This conception incorporates a number of assumptions which are listed below:

1) The different classes of views shown in fig. 10 are assumed to arise from different projections of identical particles where the tilt angle is unknown.

2) The mechanism of uranyl staining of the ν bodies is unknown. Although the method of drying the particles within stain would be expected to yield negative staining, the strong binding of uranyl ions to nucleic acids [62] could also result in positively stained regions. However, evidence employing phosphotungstic acid as a negative stain [23], and observations on unstained specimens [30], appears to justify the assumption that there is a crevice or hole in the center of the ν body.

3) Each particle is assumed to have pairs of all histones – H4, H3, H2a, H2b, and H1 or H5. The very lysine-rich histones H1 and H5 are not essential for the particulate structure [20,24,25,28,30,37,63] and probably bind to the DNA represented in the connecting strand. An octamer of the histones (H4, H3, H2a and H2b) is assumed necessary for the ν body shape [57,58].

4) All of the histones appear to consist of globular regions (~ 70 – 80 amino acid residues in length) which are assumed to be approximated to spheres of about 26 \AA diameter, and of basic tails which probably bind to the DNA [64].

5) The association of this octamer of globular regions of the histones into the protein core [65] of the ν body is assumed to follow point-group symmetry [60,61]. Of the various types of point-group symmetry for proteins with a small number of subunits [60], dihedral symmetry seems preferable to cyclic symmetry for forming the basis of a spheroid particle shape, and for maximizing histone-histone interactions. Of the two types of dihedral symmetry, the square anti-prism yields a more close-packed structure than the cubic arrangement [60]. Fig.

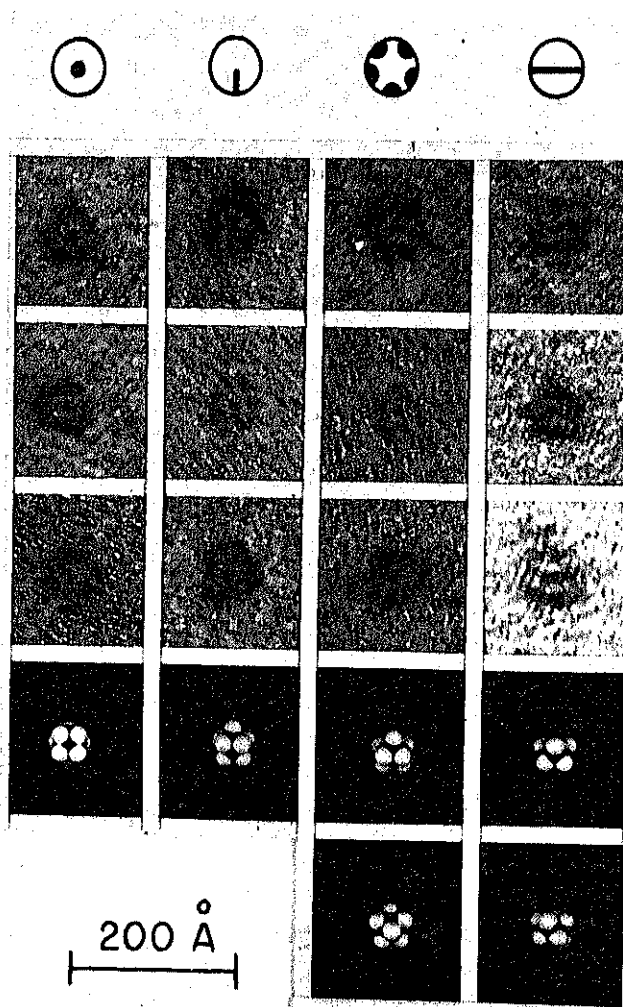
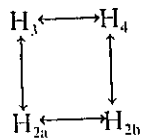


Fig. 10. A gallery of high resolution electron microscopic views of monomer v bodies, and a simulation of these views with a square antiprism arrangement of spheres. Four classes of views have been observed: particles with a dot of stain in the center; with a line of stain connecting the center and edge; a line across the diameter; and star-like patterns of stain on the periphery of the v body. Each vertical column illustrates selected representatives of each class, together with a simulation of that class by photographing tilted views of the suggested model. The monomer v bodies were applied to charged carbon-coated grids and dried in aqueous 0.2% uranyl acetate as previously described [23]. 1,200,000 \times .

10 shows photographs of a square antiprism arrangement of spheres tilted at various angles to simulate the observed electron microscopic views. A calculation of various projections [61,66] would be a more effective method for simulating

the microscopic images, and determining if the square antiprism gives a better fit than the cubic arrangement.

6) There is increasing evidence that the four different histones H4, H3, H2a, and H2b can form a specific tetramer [67], which may be assumed to be the protomer (or asymmetric unit) of the ν body. Studies of the interactions of histones in solution has led to representation of a possible arrangement of the histones in the tetramer [68]:



7) Of all the published results of chemical cross-linking of intact chromatin [35,69,70,71,72,73,74,75,76] the only identified homopolymeric link (excepting the homopolymers of H1 or H5 [69,71,72,73,75]) is H3-H3 [75,77]. We suggest that the ν body has a single dyad axis perpendicular to a pseudo four-fold axis. This dyad axis is assumed to pass between the pairs of H3.

A scheme incorporating these assumptions is presented in fig. 11, which illustrates one possible arrangement of the globular portions of the histones into a protein core. The folding of the DNA and its association with the basic regions of the histones remain unspecified, but is assumed to preserve a single

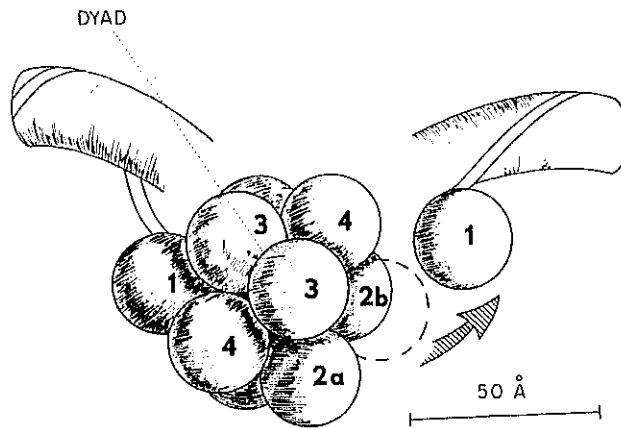


Fig. 11. Schematic conception of one possible square antiprism arrangement of histones in a protein core of the ν body. A single dyad axis is shown passing between the H3-H3 contact. The interaction of a pair of H1 (or H5) histones with the octamer (pairs of H4, H3, H2a and H2b) is shown in a 'close-packed' (left side) and in a 'stretched' (right side) configuration. The H1 (or H5) histones are also indicated to bind to the portion of the DNA represented in the connecting strand. The path of the DNA in the ν body is not indicated, but might be assumed to preserve the postulated overall two-fold axis of symmetry.

dyad axis of symmetry for the intact ν body. We are currently engaged in studying individual ν bodies at various known tilt angles in an effort to test the first of the many assumptions in this conception of the ν body.

Higher order packing of ν bodies

The problem of packaging a meter of DNA into micron size chromosomes is only partially resolved by the folding of DNA within the individual ν body. Evidence suggests that the length of DNA associated with one ν body represents a 6-7/1 compacting of the DNA [11,21,28,29,32,57]. Measurements of 200–250 Å wide chromatin fibers suggest a DNA packing ratio of $\sim 28/1$ [78]. The folded-fiber model of chromosomes has been suggested as a mechanism for additional compaction [79]. Clearly, a hierarchy of chromatin organization remains to be analyzed at the structural level.

We have been concerned with the possible arrangement of the ν bodies within both the ~ 100 and the 200–250 Å chromatin fibers. Given the structural restraints of the DNA packing ratios, fiber diameters and low-angle X-ray reflections (i.e., $\sim 110, 55, 37, 27, 22$ Å) as a basis of comparison to computations, we have calculated the properties of various arrays of ν bodies in close contact [80].

The following classes of linear particle arrays were considered (fig. 12).

Linear strings (fig. 12a). A periodic linear array of touching spheres.

Flexible strings (fig. 12b). The amount of flexibility is defined by two angles α and ψ which are randomly generated for each sphere. When the maximum value α can assume is specified (α_{\max}), then $-\alpha_{\max} \leq \alpha \leq \alpha_{\max}$. The angle ψ is a torsion angle and has a value between 0 and 2π radians. A linear string results when $\alpha_{\max} = 0^\circ$.

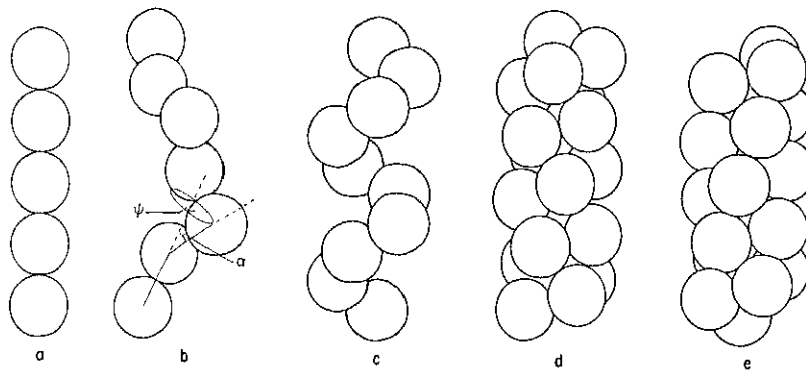


Fig. 12. Classes of models of linear arrays of spherical particles in contact: a) a linear string; b) a flexible string; c) a 2-contact helix; d) a 4-contact [1,4] helix; e) a 6-contact [1,3,4] helix.

2-Contact helices (fig. 12c). These are open helices with each sphere in contact with only the two neighboring spheres along the strand. As long as spheres do not overlap, any three of the four variables (turn angle, rise/sphere, helix radius, and sphere diameter) are independent. There is no stabilization arising from interactions of spheres other than those interactions between covalently-linked neighbors.

4-Contact helices (fig. 12d). Each sphere is in contact with spheres above and below, as well as with adjacent spheres along the strand. According to the notation of Erickson [81] these would correspond to the (l, n) helices with $n = 2, 3, 4$, etc. For each n there is a range of allowable turn angles. Only two of the four variables described above are independent.

6-Contact helices (fig. 12e). This class has the tightest structure of all of the helices. The spheres are hexagonally packed on the surface of the helix, each sphere being in contact with six other spheres. Erickson [81] calls these (l, m, n) helices, where m and n are integers limited by the previously described constraints to be: $m = 2, 3, 4$, etc. and $n = m + 1$. For a given sphere size and integer m , the helix parameters are unique.

We have also calculated the spherically averaged diffraction from the following three-dimensional close-packing arrays: cubic close-packing, face-centered cubic close-packing, body-centered cubic close-packing, and hexagonal close-packing.

Since almost nothing is known about the internal structure of an individual v body (i.e., the three-dimensional electron density distribution $\rho(r, \theta, \psi)$), we have used spherically symmetric electron density distribution $\rho(r)$ to represent them. In most calculations we have used uniform-density spheres ($\rho(r) = \text{constant}$), but have tried several other electron density distributions as well.

The Debye equation [82] was employed to calculate the spherically averaged scattering of X-rays by such model arrays of v bodies. Strictly speaking, such scattering calculations should not be compared with data from oriented chromatin fibers. However, the data from unoriented gels is very similar, and only the 110 Å reflection exhibits more than very weak meridional orientation in chromatin fibers [83].

A partial summary of our calculations of model arrays is presented in table 4. Based upon these calculations, the following general statements can be made: (a) For several quite different arrays of ~ 100 Å-diameter spherically symmetric particles, X-ray maxima are predicted at positions in agreement with the experimental positions. (b) The first maximum is due to the periodic arrangement of these particles. It occurs at an equivalent Bragg spacing approximately equal to the principal interparticle distance. The additional small-angle maxima reflect both this periodicity and the particle structure factor, the latter being dominant. A recent neutron-scattering study has likewise indicated that only the ~ 110 Å maximum is primarily attributable to the particle array [65]. (c) Both the diameter of the spheres and the principal interparticle distance must be ~ 110 Å to have

TABLE 4

Calculated parameters for certain linear arrays of 110-Å spheres.

Model	Fiber diameter (Å)	Turn angle (°)	DNA packing ratio	Bragg Spacings 110,55,37,27,22Å
Linear string	110	—	6.4	Yes
Flexible string ($z_{\max} = 0-30$)	110	—	6.4	Yes
Helix models				
2-Contact	220	130	15.1	Yes
	220	90	9.0	No
	250	90	14.6	No
4-Contact				
(1,2)*	205-225	180.0-131.8	13.7-20.1	Some**
(1,3)	225-250	131.8-97.7	20.1-27.1	Yes
(1,4)	250-283	97.7-77.4	27.1-34.1	Some**
6-Contact				
(1,2,3)	225	131.8	20.1	Yes
(1,3,4)	250	97.7	27.1	Yes
(1,4,5)	283	77.4	34.1	No

* Helix notation as developed by Erikson [81].

** Some of the helices within this class give the correct spacings.

all of the maxima in the correct positions. (d) For all of these models based on regular arrays of spherical particles, the calculated relative intensities fall off more quickly with each Bragg angle than do published experimental data, unless the scattering is greatest by the outer portion of the particle. For example, much better agreement is obtained using a core surrounded by a shell of higher effective electron density or using a three shell model (i.e. a central 'hole', a 'protein' core, and a 'DNA-rich' outer shell).

The calculated properties of these various arrays lead us to suggest the possibility that the ~ 100 Å fiber could be presented as linear or flexible strings of close-packed particles; whereas the 200-250 Å fiber could correspond to a number of possible helical arrangements (e.g., [1,2,3], [1,3,4], or [1,3]) of v bodies.

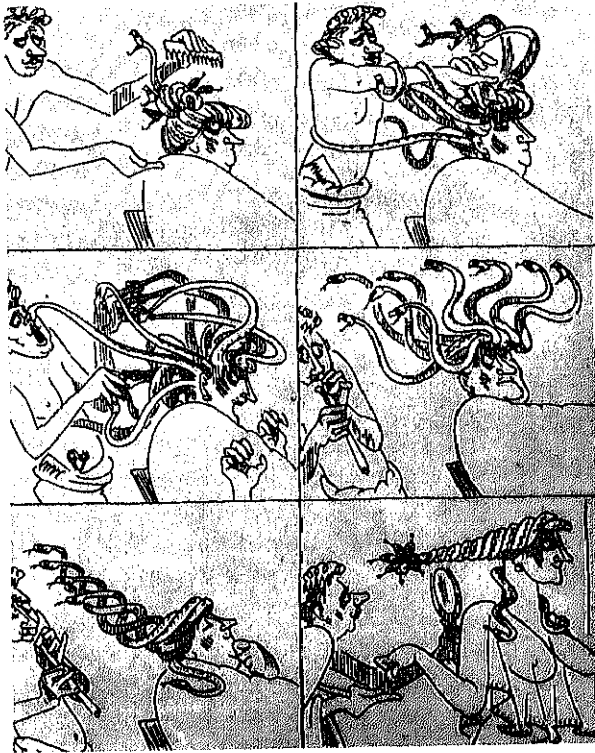


Fig. 13. Medusa at the Hairdresser. Simplicissimus (1927).

Historical perspective

A diagrammatic representation of the recent history of chromatin structure is presented in fig. 13. Anyone who has worked with isolated chromatin will recognize the value of its analogy with Medusa. The implication, from this figure, that chromatin possesses a helical structure, represents an unfortunate consequence of artistic license.

Acknowledgements

The authors wish to express their appreciation to M.H. Hsie and J. Brantley for important assistance in various phases of these studies. Dr. J.R. Einstein has helped to sharpen our awareness of the consequences of point-group symmetry. This research was sponsored by the Energy Research and Development

Administration under contract with Union Carbide Corporation, by National Institute of General Medical Science research grant GM 19334 to D.E.O., post-doctoral fellowship GM 55247 to R.D.C., and by National Institute of Child Health and Development postdoctoral fellowship HD 00436 to M.B.S.

References

- [1] M.H.F. Wilkins, Physical studies of the molecular structure of deoxyribose nucleic acid and nucleoprotein. *Cold Spring Harbor Symposium*, XXI, 75-90 (1956).
- [2] M.H.F. Wilkins, G. Zubay and H.R. Wilson, X-ray diffraction studies of the molecular structure of nucleohistone and chromosome. *J. Mol. Biol.* 1, 179-185 (1959).
- [3] V. Luzzati and A. Nicolaieff, Etude par diffusion des rayons x aux angles des gels d'acide désoxyribonucleique et de nucleoprotéines. *J. Mol. Biol.* 1, 127-133 (1959).
- [4] V. Luzzati and A. Nicolaieff, The structure of nucleohistones and nucleoprotamines. *J. Mol. Biol.* 7, 142-163 (1963).
- [5] J.F. Pardon and M.H.F. Wilkins, A super-coil model for nucleohistone. *J. Mol. Biol.* 68, 115-124 (1972).
- [6] J.G. Gall, Chromosome fibers studied by a spreading technique. *Chromosoma* 20, 221-233 (1966).
- [7] S. Bram and H. Ris, On the structure of nucleohistone. *J. Mol. Biol.* 55, 325-336 (1971).
- [8] H. Ris, Chromosomal structure as seen by electron microscopy. in: *The Ciba Foundation Symposium* (eds. D.W. Fitzsimons and G.E.W. Wolstenholme) American Elsevier, New York, Vol. 28, 7-22 (1975).
- [9] O.L. Miller and B.R. Beatty, Visualization of nucleolar genes. *Science* 164, 995-957 (1969).
- [10] O.L. Miller, B.A. Hamkalo and C.A. Thomas, Visualization of bacterial genes in action. *Science* 169, 392-395 (1970).
- [11] A.L. Olins and D.E. Olins, Spheroid chromatin units (ν Bodies). *J. Cell. Biol.* 59 (2, Pt. 2), 252a (1973).
- [12] C.L.F. Woodcock, Ultrastructure of inactive chromatin. *J. Cell. Biol.* 59 (2, Pt. 2), 368a (Abstr.) (1973).
- [13] D.R. Hewish and L.A. Burgoyne, Chromatin sub-structure. The digestion of chromatin DNA at regularly spaced sites by a nuclear deoxyribonuclease. *Biophys. Biochem. Res. Commun.* 52, 504-510 (1973).
- [14] R. Rill and K.E. Van Holde, Properties of nuclease-resistant fragments of calf thymus chromatin. *J. Biol. Chem.* 248, 1080-1083 (1973).
- [15] H. Ris and A.E. Mirsky, The state of the chromosomes in the interphase nucleus. *J. Gen. Physiol.* 32, 489-502 (1949).
- [16] N.G. Anderson and K.M. Wilbur, Studies on isolated cell components. IV. The effects of various solutions on the isolated rat liver nucleus. *J. Gen. Physiol.* 35, 781-796 (1952).
- [17] J.St. L. Philpot and J.E. Stanier, The choice of the suspension medium for rat-liver-cell nuclei. *Biochem. J.* 63, 214-223 (1956).
- [18] D.E. Olins and A.L. Olins, Physical studies of isolated eucaryotic nuclei. *J. Cell Biol.* 53, 715-736 (1972).
- [19] K. Brasch, V.L. Seligy and G. Setterfield, Effects of low salt concentration on structural organization and template activity of chromatin in chicken erythrocyte nuclei. *Exp. Cell. Res.* 65, 61-72 (1971).
- [20] A.L. Olins and D.E. Olins, Unpublished observations.
- [21] A.L. Olins and D.E. Olins, Spheroid chromatin units (ν bodies). *Science* 183, 330-332 (1974).

- [22] A.L. Olins, R.D. Carlson and D.E. Olins, Visualization of chromatin substructure: ν bodies. *J. Cell. Biol.* 64, 528-537 (1975).
- [23] A.L. Olins, M.B. Senior and D.E. Olins, Ultrastructural features of chromatin ν bodies. *J. Cell. Biol.* (1976) in press.
- [24] C.L. Woodcock, D.L. Maguire and J.E. Stanchfield, Further evidence for a structural repeating unit in chromatin. *J. Cell. Biol.* 63 (2 Pt. 2), 377a (1974).
- [25] K.E. Van Holde, C.G. Sahasrabudhe, B.R. Shaw, E.F.J. Van Bruggen and A.C. Arnberg, Electron microscopy of chromatin subunit particles. *Biochem. Biophys. Res. Commun.* 60, 1365-1370 (1974).
- [26] G.D. Howze, A.W. Hsieh and A.L. Olins, ν Bodies in mitotic chromatin. Submitted for publication.
- [27] J.B. Rattner, A.D. Branch and B.A. Hamkalo, Ultrastructure of mitotic and interphase chromosomes. *J. Cell. Biol.* 67 (2, Pt. 2), 355a (1975).
- [28] P. Oudet, M. Gross-Bellard and P. Chambon, Electron microscopic and biochemical evidence that chromatin structure is a repeating unit. *Cell* 4, 281-300 (1975).
- [29] J.D. Griffith, Chromatin structure deduced from a minichromosome. *Science* 187, 1202-1203 (1975).
- [30] J.P. Langmore and J.C. Wooley, Chromatin architecture: investigation of a subunit of chromatin by dark field electron microscopy. *Proc. Natl. Acad. Sci. U.S.A.* 72, 2691-2695 (1975).
- [31] W.E. Hill, G.P. Rossetti and K.E. Van Holde, Physical studies of ribosomes from *Escherichia coli*. *J. Mol. Biol.* 44, 263-277 (1969).
- [32] M.B. Senior, A.L. Olins and D.E. Olins, Chromatin fragments resembling ν bodies. *Science* 187, 173-176 (1975).
- [33] R.J. Clark and G. Felsenfeld, Structure of chromatin. *Nature New Biol.* 229, 101-106 (1971).
- [34] M. Noll, Subunit structure of chromatin. *Nature* 251, 249-251 (1974).
- [35] F. Van Lente, J.F. Jackson and H. Weintraub, Identification of specific crosslinked histones after treatment of chromatin with formaldehyde. *Cell* 5, 45-50 (1975).
- [36] D.K. Oosterhof, J.C. Hozier and R.L. Rill, Nuclease action on chromatin: evidence for discrete, repeated nucleoprotein units along chromatin fibrils. *Proc. Natl. Acad. Sci. U.S.A.* 72, 633-637 (1975).
- [37] V.V. Bakayev, A.A. Melnickov, V.D. Osicka and A.J. Varshavsky, Studies on chromatin. II. Isolation and characterization of chromatin subunits. *Nucleic Acids Res.* 2, 4101-4119 (1975).
- [38] C.T. Rankin, N.G. Anderson and W.L. Rasmussen, Improvement of methods for macroglobulin isolation in B-XV and B-XXVII Rotors. USAEC Report ORNL-4171, 65-72 (1967).
- [39] S.P. Spragg, R.S. Morrod and C.T. Rankin, The optimization of density gradients for zonal centrifugation. *Separation Sci.* 4, 467-481 (1969).
- [40] W.K. Sartory, H.B. Halsall and J.P. Breittatt, Simulation of gradient and band propagation in the centrifuge. In the *Proc. of 50th Anniversary Conf. of the Ultracentrifuge*, Bethesda, Maryland. *Biophys. Chem.* (1975) in press.
- [41] N.G. Anderson, D.A. Waters, C.E. Nunley, R.F. Gibson, R.M. Schilling, E.C. Denny, G.B. Cline, E.F. Babelay and T.E. Perardi, K-Series centrifuges. I. Development of the K-II continuous-sample-flow-with-banding centrifuge system for vaccine purification. *Anal. Biochem.* 32, 460-464 (1969).
- [42] N.G. Anderson and E. Rutenberg, Analytical techniques for cell fractions. VII. A simple gradient-forming apparatus. *Anal. Biochem.* 21, 259-265 (1967).
- [43] B.M. Honda, D.L. Baillie and E.P.M. Candido, Properties of chromatin subunits from developing trout testis. *J. Biol. Chem.* 250, 4643-4647 (1975).
- [44] B. Sollner-Webb and G. Felsenfeld, A comparison of the digestion of nuclei and chromatin by staphylococcal nuclease. *Biochemistry* 14, 2915-2920 (1975).
- [45] R. Axel, Cleavage of DNA in nuclei and chromatin with staphylococcal nuclease. *Biochemistry* 14, 2921-2925 (1975).

- [46] L.A. Burgoyne, D.R. Hewish and J. Mobbs, Mammalian chromatin substructure studies with the calcium-magnesium endonuclease and two-dimensional polyacrylamide-gel electrophoresis. *Biochem. J.* 143, 67-72 (1974).
- [47] B.R. Shaw, J.L. Corden, C.G. Sahasrabudde and K.E. Van Holde, Chromatographic separation of chromatin subunits. *Biophys. Biochem. Res. Commun.* 61, 1193-1198 (1974).
- [48] J.D. McGhee and J.D. Engel, Subunit structure of chromatin is the same in plants and animals. *Nature* 254, 449-450 (1975).
- [49] D. Lohr and K.E. Van Holde, Yeast chromatin subunit structure. *Science* 188, 165-166 (1975).
- [50] M.B. Senior and D.E. Olins, Unpublished observations.
- [51] R.J. Clark and G. Felsenfeld, Chemical probes of chromatin structure. *Biochemistry* 13, 3622-3628 (1974).
- [52] R. Axel, W. Melchoir, B. Sollner-Webb and G. Felsenfeld, Specific sites of interaction between histones and DNA in chromatin. *Proc. Natl. Acad. Sci. U.S.A.* 71, 4101-4105 (1974).
- [53] H. Weintraub and F. Van Lente, Dissection of chromosome structure with trypsin and nucleases. *Proc. Natl. Acad. Sci. U.S.A.* 71, 4249-4253 (1974).
- [54] E.B. Wright and D.E. Olins, Histone stoichiometry in chicken erythrocyte nuclei. *Biophys. Biochem. Res. Commun.* 63, 642-650 (1975).
- [55] S. Panyim and R. Chalkley, The heterogeneity of histones. I. A quantitative analysis of calf histones in very long polyacrylamide gels. *Biochemistry* 8, 3972-3979 (1969).
- [56] S. Panyim, D. Bilek and R. Chalkley, An electrophoretic comparison of vertebrate histones. *J. Biol. Chem.* 246, 4206-4215 (1971).
- [57] R.D. Kornberg, Chromatin structure: a repeating unit of histones and DNA. *Science* 184, 865-868 (1974).
- [58] K.E. Van Holde, C.G. Sahasrabudde and B.R. Shaw, A model for particulate structure in chromatin. *Nucleic Acids Res.* 1, 1579-1586 (1974).
- [59] E.W. Jones and S. Forrester, Interactions between the lysine-rich histone F1 and deoxyribonucleic acid. *Biochem. J.* 111, 371-374 (1969).
- [60] I.M. Klotz, D.W. Darnall and N.R. Langerman, Quaternary structure of proteins, in: *The Proteins*, 3rd edition (ed., H. Neurath and R.L. Hill), Academic Press, Inc., New York. Volume 1, 294-411 (1974).
- [61] J.T. Finch, Electron microscopy of proteins, in: *The Proteins*, 3rd edition (ed., H. Neurath and R.L. Hill), Academic Press, Inc., New York. Volume 1, 413-497 (1974).
- [62] C.R. Zobel and M. Beer, Chemical studies on the interaction of DNA with uranyl salts. *J. Biophys. Biochem. Cytol.* 10, 335-346 (1961).
- [63] R.D. Kornberg and J.O. Thomas, Chromatin structure: oligomers of histones. *Science* 184, 865-868 (1974).
- [64] E.M. Bradbury, Histones in chromosomal structure and control of cell division. In the Ciba Foundation Symposium (eds., D.W. Fitzsimons and G.E.W. Wolstenholme) American Elsevier, New York. Volume 28 131-149 (1975).
- [65] J.P. Baldwin, P.G. Boseley, E.M. Bradbury and K. Ibel, The subunit structure of the eukaryotic chromosome. *Nature* 253, 245-249 (1975).
- [66] R. Josephs, Electron microscopic studies on glutamic dehydrogenase: subunit structure of individual molecules and linear associates. *J. Mol. Biol.* 55, 147-153 (1971).
- [67] H. Weintraub, K. Palter and F. Van Lente, Histones H2a, H2b, H3 and H4 form a tetrameric complex in solutions of high salt. *Cell* 6, 85-110 (1975).
- [68] J.A. D'Anna and I. Isenberg, A histone cross-complexing pattern. *Biochemistry* 13, 4992-4997 (1974).
- [69] D.E. Olins and E.B. Wright, Glutaraldehyde fixation of isolated eucaryotic nuclei. *J. Cell. Biol.* 59, 304-317 (1973).

- [70] H.G. Martinson and B.J. McCarthy, Histone-histone associations within chromatin. Cross-linking studies using tetranitromethane. *Biochemistry* 14, 1073-1078 (1975).
- [71] R. Chalkley and C. Hunter, Histone-histone propinquity by aldehyde fixation of chromatin. *Proc. Natl. Acad. Sci. U.S.A.* 72, 1304-1308 (1975).
- [72] R. Chalkley, Histone propinquity using imidoesters. *Biochem. Biophys. Res. Commun.* 64, 587-594 (1975).
- [73] W.M. Bonner and H.B. Pollard, The presence of F3-F2al dimers and F1 oligomers in chromatin. *Biochem. Biophys. Res. Commun.* 64, 282-288 (1975).
- [74] J.E. Hyde and I.O. Walker, Covalent cross-linking of histones in chromatin. *FEBS Letters* 50, 150-154 (1975).
- [75] R.C. Hardison, M.E. Eichner and R. Chalkley, An approach to histone nearest neighbors in extended chromatin. *Nucleic Acid Res.* 2 1751-1770 (1975).
- [76] Y.V. Ilyin, A.A. Bayer, A.L. Zhuze and A.J. Varshavsky, Histone-histone proximity in chromatin as seen by imidoester cross-linking. *Mol. Biol. Rep.* 1, 343-348 (1974).
- [77] J.O. Thomas and R.D. Kornberg, An octamer of histones in chromatin and free in solution. *Proc. Natl. Acad. Sci. U.S.A.* 72, 2626-2630 (1975).
- [78] H.M. Golomb and G.F. Bahr, Electron microscopy of human interphase nuclei. Determination of total dry mass and DNA-packing ratio. *Chromosoma* 46, 233-245 (1974).
- [79] E.J. DuPraw, Macromolecular organization of nuclei and chromosomes: a folded fibre model based on whole-mount electron microscopy. *Nature*, 206, 338-342 (1965).
- [80] R.D. Carlson and D.E. Olms, Chromatin model calculations: arrays of spherical v bodies (1976) submitted for publication.
- [81] R.O. Erickson, Tubular packing of spheres in biological fine structure. *Science* 181, 705-716 (1973).
- [82] P. Debye, Zerstreung von Röntgenstrahlen. *Ann. Physik.* 46, 809-823 (1915).
- [83] B.M. Richards and J.F. Pardon, The molecular structure of nucleohistone (DNH). *Exp. Cell. Res.* 62, 184-196 (1970).